Chemical Physics Letters 783 (2021) 139071

Contents lists available at ScienceDirect

Chemical Physics Letters

journal homepage: www.elsevier.com/locate/cplett

Research paper

Cuprous oxide induced the surface enhanced Raman scattering of silver thin films

Tingting Liu [a], Qingyou Liu [b], Ruijin Hong [a,*], Chunxian Tao [a], Qi Wang [a], Hui Lin [a], Zhaoxia Han [a], Dawei Zhang [a]

[a] Engineering Research Center of Optical Instrument and System, Ministry of Education and Shanghai Key Lab of Modern Optical System, University of Shanghai for Science and Technology, No.516 Jungong Road, Shanghai 200093, China
[b] Key Laboratory of High-temperature and High-pressure Study of the Earth's Interior, Institute of Geochemistry, Chinese Academy of Sciences, Guiyang 550081, China

ARTICLE INFO

Keywords:
Cu_2O-Ag composite films
Localized surface plasmons
Raman scattering intensity
Various molecules

ABSTRACT

In this work, silver thin films with various thicknesses deposited on cuprous oxide (Cu_2O) buffer layer were obtained. XRD and AFM results show that the Cu_2O buffer layer has the effect of improving the surface quality and crystallinity of the Cu_2O-Ag composite films. The coupling between Cu_2O and localized surface plasmons of the silver thin films was investigated by optical absorption and Raman scattering experiments. The absorption spectra showed that the intensity of Cu_2O/Ag composite thin films was increased and shifted from the visible to the near-infrared region with an increase of the silver layer thickness. Compared with single-layer sample, the Raman scattering intensity of Cu_2O/Ag composite was increased by 19.97 and 1.48 times, respectively. By the FDTD simulation of single layer and composite films, the electric field enhancement characteristics of the composite structure are confirmed. At the same time, the composite also exhibits good property as a SERS substrate for probing various molecules such as RhB, MB, and R6G.

1. Introduction

Surface Enhanced Raman Scattering (SERS) is widely used in biological analysis and other fields because of its high sensitivity, good selectivity and high stability for adsorbates. Generally, there are two main mechanisms commonly used to explain SERS enhancement: electromagnetic enhancement and chemical enhancement. The electromagnetic enhancement is mainly caused by the local plasmon resonance of the sample, and its enhancement factor is as high as 10^{14} [1]. The chemical bond formed between the molecule and the SERS substrate or the charge transfer induced by the complex is usually the reason for the chemical enhancement, but its enhancement effect is weaker and the enhancement factor is only 10^3. Due to the strong electromagnetic enhancement of precious metals and the excellent chemical enhancement capabilities of semiconductors, researchers have turned their attention to SERS substrates where precious metals and semiconductors are compounded [2,3]. For example, flower-shaped molybdenum disulfide-Ag nanoparticles are used for the detection of tetramethylthiuram disulfide (TMTD) through the SERS effect induced by charge transfer resonance [4]. The integrated SERS substrate of TiN plasma antenna and Si waveguide is used for electromagnetic resonance research [5].

As a typical p-type semiconductor material with a band gap of about 2.17 eV, Cu_2O can be excited by the visible light in the wavelength range of 300–700 nm to generate electron-hole pair, so it has a broad application prospect in the fields of photocatalyzation [6], electrochemistry [7], SERS [8] and so on. In 1998, Kudelski and co-workers [9] reported for the first time that Cu_2O can be used as a SERS substrate. In 2013, Jiang et al. [10] reported that Cu_2O nanospheres enhanced the Raman signal of 4-mercaptobenzoic acid molecules. In recent years, Lin et al. [11] have studied the influence of Cu_2O crystallites with different phases on SERS activity. Although the preparation of single-phase Cu_2O semiconductor with various morphologies is relatively simple, its role in enhancing SERS activity is weak, so it is usually modified by the deposition of precious metals (Au, Pt, Ag) [12–14]. Compared with Au and Pt, Ag is a relatively cheap precious metal. Therefore, it is very necessary to study the modification of nano-Cu_2O SERS substrate by precious metal Ag. In 2014, Yang et al. prepared Ag NPs-modified cuprous oxide highly sensitive SERS substrates by a simple one-pot method with an enhancement factor of about 10^5 [15]. Subsequently, Ag@Cu_2O

* Corresponding author.
E-mail address: rjhong@usst.edu.cn (R. Hong).

https://doi.org/10.1016/j.cplett.2021.139071
Received 4 July 2021; Received in revised form 17 September 2021; Accepted 19 September 2021
Available online 21 September 2021

core–shell nanoparticles introduced a plasmon resonance mechanism to effectively improve the SERS effect of 4-MBA adsorbed on the particles [16]. Recently, Sheng et al. [17] prepared Ag NPs-attached cuprous oxide nanospheres by chemical reduction and confirmed that the strong electric field coupling and plasmon resonance effect are the reasons for the high SERS performance of Rhodamine 6G. At present, Cu_2O/Ag SERS substrates are mainly prepared by chemical methods. The synthesis process requires special equipment and the nanoparticles are prone to agglomeration. At the same time, the probe molecule used for detection is relatively single, and it is necessary to improve the preparation method of Cu_2O/Ag active substrate and detect a variety of probe molecules to verify the SERS performance.

In this paper, we report a simple and effective method for preparing Cu_2O/Ag SERS active substrates. The cuprous oxide film was prepared by thermal oxidation, and Ag nanoparticles were deposited by electron beam evaporation. X-ray diffraction patterns and ultraviolet–visible absorption spectra were used to study the changes in the material composition and optical properties of Cu_2O-Ag nanocomposites. By changing the thickness of the Ag layer, we explored the most suitable Cu_2O-Ag heterojunction as the SERS substrate. In addition, Methylene Blue (MB), Rhodamine B and R6G were used as probe molecules to study the SERS activity and uniformity of Cu_2O-Ag composite samples.

2. Experimental

The cuprous oxide film is obtained by first growing a Cu film from a copper target (99.99%) on a K9 glass substrate by electron beam evaporation, and then placing it in a home-made tube furnace (200℃) for heat treatment for 2 h. The glass substrate was ultrasonically cleaned in acetone, ethanol, and deionized water for 15 min before deposition, and then dried in nitrogen. The thickness of the Cu_2O film is 60 nm. Next, an Ag layer was deposited on the Cu_2O film by electron beam evaporation, with thicknesses of 5, 10, and 15 nm, respectively. The specific preparation process of the Cu_2O-Ag composite samples are shown in Fig. 1. The thickness of all films is monitored by an in-situ quartz crystal microbalance. At the same time, an Ag nano-film was deposited on the blank substrate as a contrast sheet.

The structural properties and the crystallinity of the samples are characterized by X-ray diffraction (XRD) using a Bruker AXS/D8 Advance system, with Cu Ka radiation ($\lambda = 0.15408$ nm). The surface morphology of the samples was characterized by atomic force microscope (AFM)(XE-100, Park System) with a 3 μm × 3 μm scanning area. The UV–VIS-NIR double beam spectrophotometer (Lambda1050, PerkinElmer, USA) is used to measure the optical absorption spectrum of samples, with the scanning range of 250 ~ 1200 nm and a step length of 2 nm. Raman scattering spectra are acquired from a confocal microprobe Raman system (inVia Raman Microscope, Renishaw) with 633 nm laser excitation. All samples are tested at room temperature.

3. Results and discussion

Fig. 2 shows the XRD patterns of as-annealed pure cuprous oxide, as-deposited silver and Cu_2O-Ag composite film samples with different Ag layers. In pure cuprous oxide, only a diffraction peak appears near 37.4°, corresponding to the (1 1 1) crystal plane of Cu_2O crystal (JCPDS No. 34–1354). No diffraction peaks are observed in the Ag film sample, which indicates that the film thickness is too thin and the atoms on the surface are randomly arranged, resulting in the amorphous state of the Ag film [18]. For the Cu_2O-Ag composite sample, the Cu_2O (1 1 1) peak and a new diffraction peak corresponding to the (1 1 1) plane of Ag (JCPDS No. 04–0783) around 39.1° coexist, confirming the successful synthesis of the Cu_2O-Ag composite films. It is because the thickening of the Ag film effectively improves the surface quality of the film and modifies the underlying cuprous oxide [19,20].

The AFM images with the scanning area of 3 μm × 3 μm for all samples are shown as Fig. 3(a-e). The as-deposited Ag film is relatively uniform, dense and orderly, and its surface roughness root mean square (RMS) value is only 1.49. The surface roughness of as-annealed cuprous oxide increases to 5.13 due to the aggregation of heat-affected particles. Fig. 3(c-e) show the AFM images of Cu_2O-Ag composite samples with Ag thicknesses of 5, 10, and 15 nm. Because of the influence of the Cu_2O base film and the inter-doping of atoms on the heterojunction interface into the lattice [21], the surface roughness of the composite film increased to 12.23, 7.52, and 4.98, respectively. At the same time, the surface quality of the composite film increases as the thickness of the Ag layer increases, which is attributed to the fact that the deposited Ag particles are smaller than Cu_2O and the surface is smoother [22].

Fig. 4 shows the absorption spectra of single layer Ag, Cu_2O and composite thin films. The absorption spectrum of as-annealed Cu_2O is characterized by two absorption peaks near 348 and 450 nm, which are caused by the scattering and inter-band transition in Cu_2O [23,24]. The 10 nm thick Ag film has a wide absorption band at 550 nm corresponding to the local surface plasmon resonance (LSPR) effect of Ag nanoparticles, which is similar to that reported in other literature [25]. The Cu_2O-Ag composite film effectively enhances the absorption intensity in the visible light region of 400–800 nm and enhances the absorption in the near-infrared region. The reason for this trend of change is the synergistic enhancement of the absorption of Cu_2O and Ag

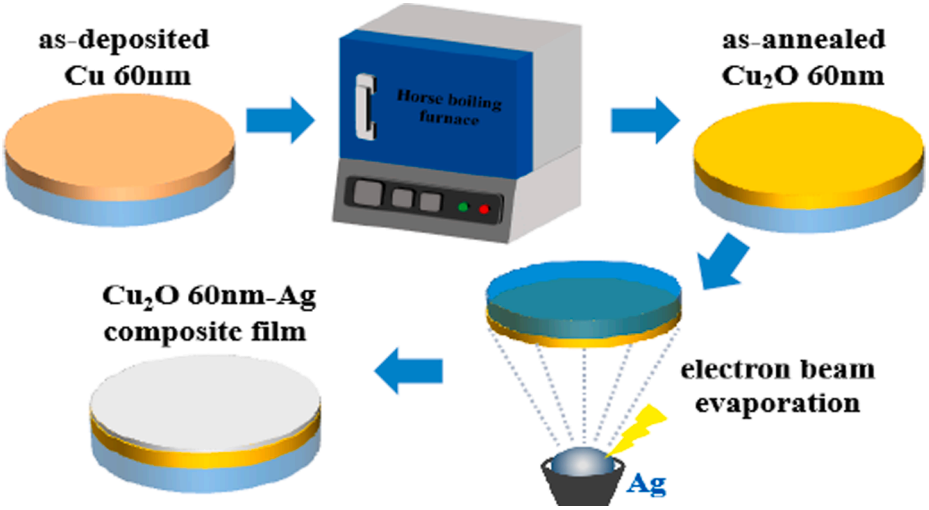

Fig. 1. The Schematic diagram of the fabrication process of Cu_2O-Ag nano-film.

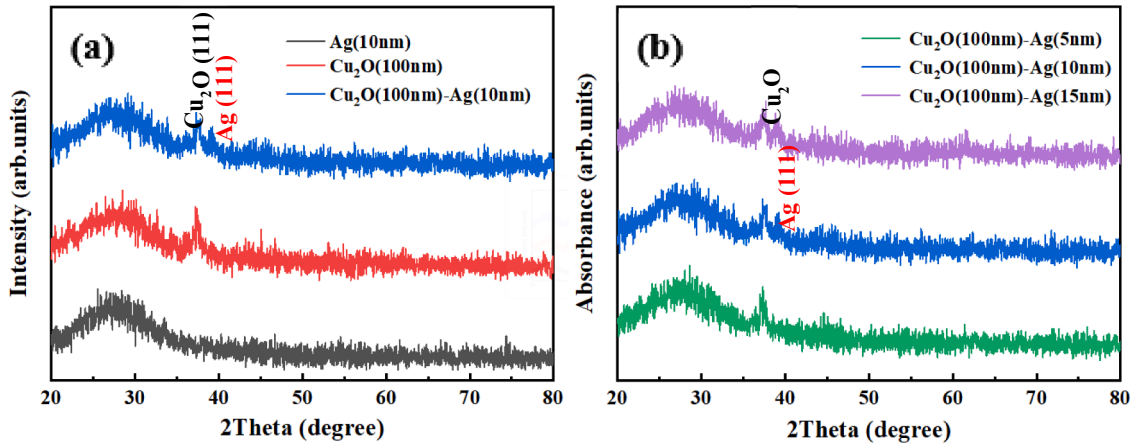

Fig. 2. The XRD patterns of (a) nano-Cu_2O, Ag thin film and (b) Cu_2O-Ag composite film samples with different Ag layer thicknesses.

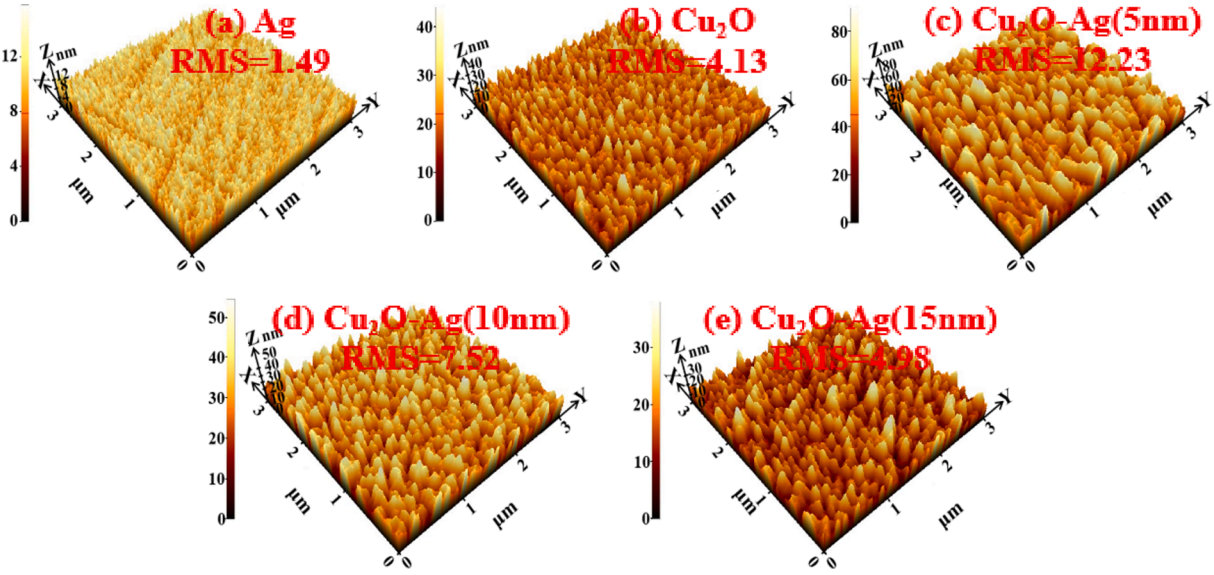

Fig. 3. AFM images of (a) Ag, Cu_2O thin film and (b) Cu_2O-Ag composite film samples with different Ag layer thicknesses.

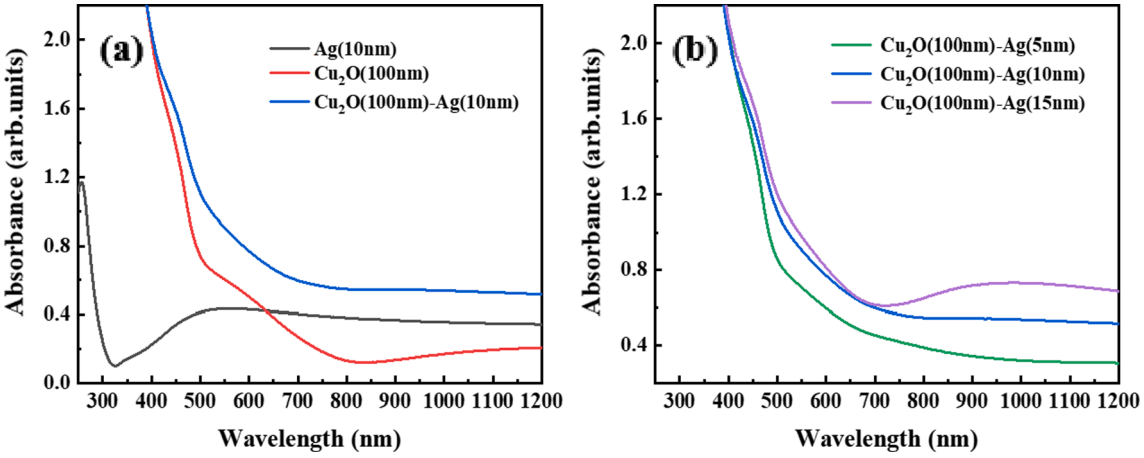

Fig. 4. The absorption spectrum of (a) Ag, Cu_2O thin film and (b) Cu_2O-Ag composite films with different Ag layer thicknesses.

particles and the plasma absorption characteristics of space-limited electrons in Ag nanoparticles [26,27]. With the thickness of the Ag layer increasing, the absorption peaks of the sample increased and shifted from the visible to the near-infrared region, and when the Ag thickness reaches 15 nm, a new diffraction peak appears near 900 nm.

In order to study the synergistic enhancement of Cu_2O and Ag particles, we chose 10^{-4} mol/L RhB as the probe molecule to explore the Raman spectra of Cu_2O, Ag and Cu_2O-Ag heterojunctions. According to Fig. 5(a), both as-annealed Cu_2O and as-deposited Ag films have observed obvious Raman signals, indicating that these two substances have the ability to detect SERS as substrates. Moreover, after Cu_2O and Ag composite, they showed a more significant Raman enhancement effect, which was 19.97 and 1.48 times that of single-layer Cu_2O and Ag films, respectively. For Cu_2O-Ag composite films with different Ag layer thicknesses, the SERS performance of the samples increases as the thickness of the silver layer increases, as shown in Fig. 5(b). It is because the increase in the thickness of the Ag layer enhances the coupling between Cu_2O and Ag [15], and at the same time improves the light absorption capacity and LSPR characteristics of the composite samples [28,29]. In addition, it can be observed that there are four distinct Raman peaks at 620, 1361, 1506 and 1648 cm^{-1} in the RhB molecule, corresponding to the aromatic bending vibration and the C-C stretching vibration mode [19,30,31], respectively. In order to study the uniformity of the SERS signal obtained from the Cu_2O-Ag sample as the substrate, when detecting the 10^{-5} mol/L RhB dye solution, 20 points were randomly selected from the substrate to obtain the Raman spectrum, as shown in Fig. 5(c-d) . It is found that the 20 points obtained are relatively uniform, and the relative standard deviations of the Raman signal intensity at 620 cm^{-1} and 1648 cm^{-1} are 12.8% and 13.9%, respectively. The relative standard deviation of all calculations is less than 15%, indicating that the prepared Cu_2O-Ag Raman substrate has good reproducibility.

Fig. 6 shows as-prepared Cu_2O-Ag composite film used as a SERS substrate to detect a variety of probe molecules (such as RhB, MB, and R6G). In the SERS band of MB, significant Raman enhancements were observed at approximately 448, 1396, and 1624 cm^{-1}. These peaks correspond to the C-N-C and C-C vibration modes in the MB molecule [14,32]. In addition, the Raman peaks at 1357, 1504, and 1645 cm^{-1} corresponding to R6G molecules [17,33,34] can also be observed in Fig. 6. The above results confirm that the synthesized Cu_2O-Ag composite sample can be used as a Raman substrate to detect a variety of substances.

The metal/semiconductor SERS enhancement mechanism usually consists of two parts: electromagnetic enhancement and chemical enhancement. We use Fig. 6(b) to illustrate the enhancement mechanism of Cu_2O-Ag heterostructure in detail. In the composite structure, the Fermi levels of Cu_2O and Ag are not consistent, so the charge transfer from Ag to Cu_2O makes the Fermi levels of the two systems consistent. When we use 633 nm laser excitation, the Ag NPs in the sample absorb the incident light to generate LSPR and excite a strong electric field. This process belongs to electromagnetic enhancement. At the same time, the electrons in Ag quickly transfer to the conduction band of Cu_2O, which is a chemical enhancement. In addition, due to the interface lattice defects of the Cu_2O-Ag sample, a defect level is formed near the bottom of the Cu_2O conduction band, which can accelerate the charge transfer of the composite sample. In order to verify the electric field enhancement of the Cu_2O-Ag composite sample, we used the finite element analysis method to simulate the electric field distribution of the composite film when excited by the excitation light with a wavelength of 633 nm, as shown in Fig. 7. The surface of the single-layer cuprous oxide and silver

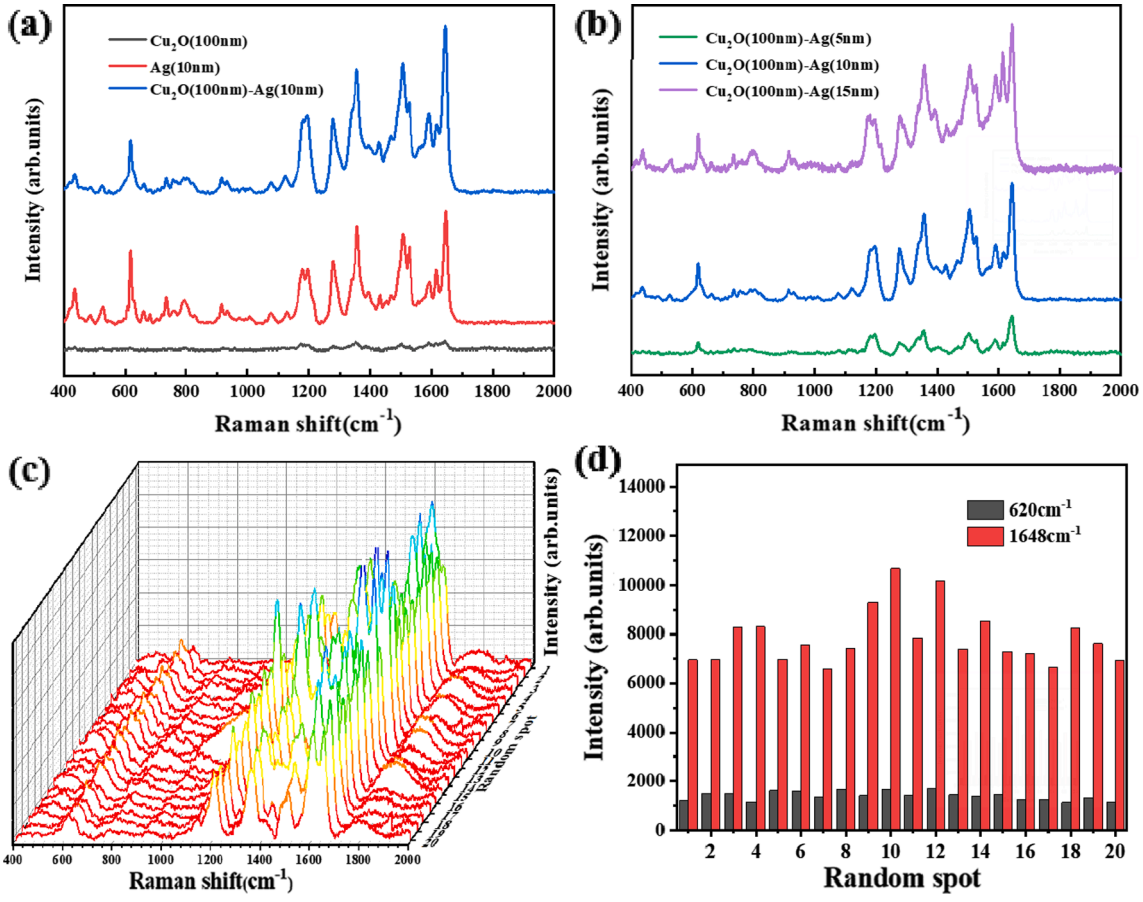

Fig. 5. Raman spectra of 10^{-4} mol/L RhB adsorbed on (a) Cu_2O, Ag and (b) Cu_2O-Ag composite films with different Ag layer thicknesses. (c) The reproducibility of 3D Raman spectra of 10^{-5} M RhB molecules at 20 different sites on Cu_2O-Ag substrate. (d) The intensity change of the peak at 620 and 1648 cm^{-1} in (c).

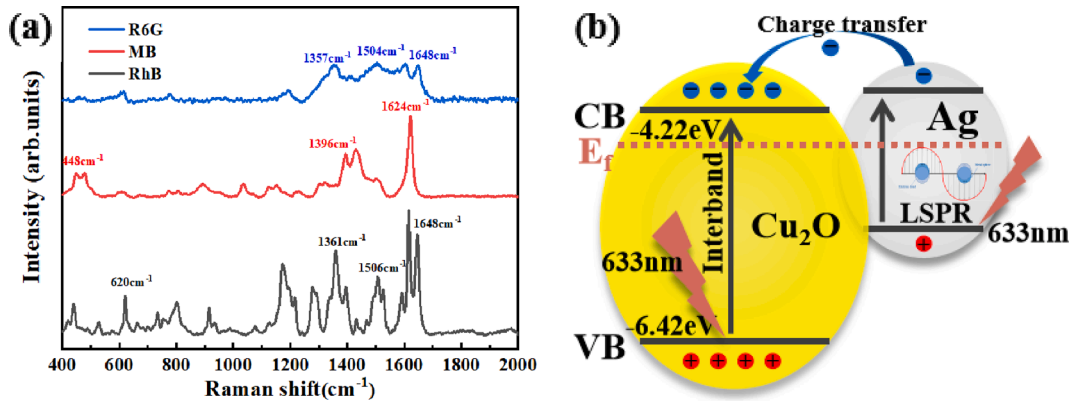

Fig. 6. (a) Raman spectra of 10^{-4} mol/L of RhB, MB and R6G probe molecules adsorbed on Cu_2O-Ag(15 nm) substrate. (b) The SERS enhancement mechanism of Cu_2O-Ag composite films when irradiated by laser with a wavelength of 633 nm.

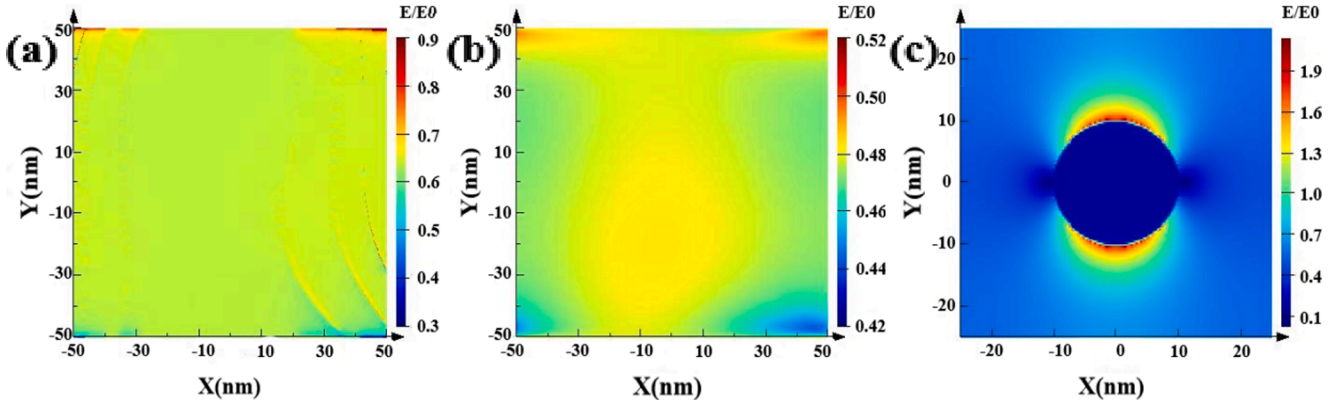

Fig. 7. FDTD simulated electric field amplitude patterns of (a) Ag, (b) Cu_2O and Cu_2O-Ag composite sample.

film is relatively uniform, and the electric field intensity is only 0.5–0.9. The surface roughness of Cu_2O and Ag increases after the combination of the two, Ag NPs aggregates, and the local electric field intensity of Cu_2O-Ag samples increases to 2.1. The FDTD results show that the synergistic effect of Cu_2O and Ag can effectively enhance the local electric field of the sample.

4. Conclusion

In conclusion, Cu_2O-Ag composite thin films were fabricated and used as Raman substrates to detect rhodamine B, methylene blue (MB) and R6G probe molecules. Compared with single-layer Cu_2O and Ag films, Cu_2O-Ag samples have good surface morphology, crystalline quality and excellent linear absorption performance. Moreover, the Cu_2O-Ag composite film exhibits a significant Raman enhancement as the result of the coupling of the electric field enhancement induced by the LSPR effect of Ag NPs and the accelerated charge transfer at the interface between Cu_2O and Ag. The FDTD simulation results of the samples and the detection of multi-probe molecules confirmed the Raman enhancement mechanism of the composite film.

CRediT authorship contribution statement

Tingting Liu: Software. **Qingyou Liu:** Software. **Ruijin Hong:** Supervision. **Chunxian Tao:** Formal analysis. **Qi Wang:** Formal analysis. **Hui Lin:** Formal analysis. **Zhaoxia Han:** Formal analysis. **Dawei Zhang:** Project administration, Validation.

Declaration of Competing Interest

The authors declare that they have no known competing financial interests or personal relationships that could have appeared to influence the work reported in this paper.

Acknowledgment

This work was supported by the National Natural Science Foundation of China (61775141, 62075133).

References

[1] X. Zhang, S. Zhang, C. Chang, Y. Feng, Y. Li, N. Dong, K. Wang, L. Zhang, W.J. Blau, J. Wang, Nanoscale 7 (2015) 2978.
[2] H. Tang, G. Meng, Q. Huang, Z. Zhang, Z. Huang, C. Zhu, Adv Funct Mater 22 (2012) 218.
[3] X. Li, G. Chen, L. Yang, Z. Jin, J. Liu, Adv Funct Mater 20 (2010) 2815.
[4] Y. Chen, H. Liu, Y. Tian, Y. Du, Y. Ma, S. Zeng, C. Gu, T. Jiang, J. Zhou, ACS Appl Mater Inter 12 (2020) 14386.
[5] J. Chen, X. Wang, F. Tang, X. Ye, L. Yang, Y. Zhang, Results Phys 16 (2020).
[6] M. Sakar, S. Balakumar, J Photoch Photobio A 356 (2018) 150.
[7] Y.C. Chen, Y.J. Chen, R. Popescu, P.H. Dong, D. Gerthsen, Y.K. Hsu, ChemSusChem 12 (2019) 4859.
[8] Y. Li, Y. Wang, M. Wang, J. Zhang, Q. Wang, H. Li, Mikrochim Acta 187 (2019) 59.
[9] A. Kudelski, W. Grochala, M. Janik-Czachor, J. Bukowska, A. Szummer, M. Dolata, J Raman Spectrosc 29 (1998) 431.
[10] L. Jiang, T. You, P. Yin, Y. Shang, D. Zhang, L. Guo, S. Yang, Nanoscale 5 (2013) 2784.
[11] J. Lin, W. Hao, Y. Shang, X. Wang, D. Qiu, G. Ma, C. Chen, S. Li, L. Guo, Small 14 (2018).
[12] W. Xu, J. Jia, T. Wang, C. Li, B. He, J. Zong, Y. Wang, H.J. Fan, H. Xu, Y. Feng, H. Chen, Angew Chem Int Edit 59 (2020) 22246.
[13] J. Jin, H. Mei, H. Wu, S. Wang, Q. Xia, Y. Ding, J Alloy Compd 689 (2016) 174.

[14] J. Zou, W. Song, W. Xie, B. Huang, H. Yang, Z. Luo, Nanotechnology 29 (2018), 115703.
[15] L. Yang, J. Lv, Y. Sui, W. Fu, X. Zhou, J. Ma, S. Su, W. Zhang, P. Lv, D. Wu, Y. Mu, H. Yang, CrystEngComm 16 (2014).
[16] L. Chen, H. Sun, Y. Zhao, Y. Zhang, Y. Wang, Y. Liu, X. Zhang, Y. Jiang, Z. Hua, J. Yang, RSC Adv 7 (2017) 16553.
[17] S. Sheng, Y. Ren, S. Yang, Q. Wang, P. Sheng, X. Zhang, Y. Liu, ACS Omega 5 (2020) 17703.
[18] R.J. Hong, W. Shao, W.F. Sun, C. Deng, C.X. Tao, D.W. Zhang, Opt Mater 77 (2018) 198.
[19] S. Ji, S. Kou, M. Wang, H. Qiu, X. Sun, J. Dou, Z. Yang, Appl Surf Sci 489 (2019) 1002.
[20] H.B. Yin, Y. Zhao, J. Li, Q. Yang, W.D. Wu, Mater Chem Phys 241 (2020).
[21] H.-Q. Liu, C.-B. Yao, G.-Q. Jiang, Y. Cai, J Alloy Compd 847 (2020).
[22] N.A. Saad, M.H. Dar, E. Ramya, R.G. Naraharisetty, D.N. Rao, J Mater Sci 54 (2019) 188.
[23] M.-Y. Kuo, C.-F. Hsiao, Y.-H. Chiu, T.-H. Lai, M.-J. Fang, J.-Y. Wu, J.-W. Chen, C.-L. Wu, K.-H. Wei, H.-C. Lin, Y.-J. Hsu, Appl Catal B-Environ 242 (2019) 499.
[24] Z. Wang, X. Liang, Y. Zhu, X. Zouhu, X. Feng, R. Zhu, Ceram Int 45 (2019) 23310.
[25] Y.-C. Fang, L. Hong, L. Wan, K.-X. Zhang, X. Lu, C.-M. Wang, J. Yang, X.-L. Xu, J Vac Sci Technol A 31 (2013).
[26] Z. Yang, C. Ma, W. Wang, M. Zhang, X. Hao, S. Chen, J Colloid Interface Sci 557 (2019) 156.
[27] J. Ma, S. Guo, X. Guo, H. Ge, Surf Coat Tech 272 (2015) 268.
[28] W. Sun, R. Hong, Q. Liu, Z. Li, J. Shi, C. Tao, D. Zhang, Opt Mater 96 (2019).
[29] S.Y. Ding, J. Yi, J.F. Li, B. Ren, D.Y. Wu, R. Panneerselvam, Z.Q. Tian, Nat Rev Mater 1 (2016).
[30] W.X. Wei, Q.L. Huang, Spectrochimica Acta A 179 (2017) 211.
[31] Y.S. Liu, W. Gao, C. Zhang, L. Zhang, Y.X. Zhi, J Taiwan Inst Chem E 88 (2018) 277.
[32] H. Dizajghorbani Aghdam, S. Moemen Bellah, R. Malekfar, Spectrochimica Acta A 223 (2019).
[33] J. Lin, Y. Shang, X. Li, J. Yu, X. Wang, L. Guo, Adv Mater 29 (2017).
[34] A.K. Pal, S. Pagal, K. Prashanth, G.K. Chandra, S. Umapathy, D.B. Mohan, Sensors Actuat B-Chem 279 (2019) 157.